Hao Wang ✉
Lin Gan

https://doi.org/10.21278/TOF.474044422
ISSN 1333-1124
eISSN 1849-1391

ANALYSIS OF SURVIVABILITY OF THE SHIP PROPULSION SYSTEM IN A SEVERE SHOCK ENVIRONMENT, BASED ON THE FUZZY THEORY AND ANALYTIC HIERARCHY PROCESS

Summary

Ship survivability is a critical aspect of the design of naval ships operating in weapon-induced shock environments. While most of studies have focused on the failure mechanisms of ship structures, little work has been done to assess the damage that may be inflicted on the propulsion systems of such vessels. This paper presents a novel model for evaluating the survivability of naval ship propulsion systems subjected to severe shock environments. The model accounts for the effects of weapon damage, including blast-induced structural crevasses and shock-induced equipment failures, by conducting the vulnerability analysis using empirical formulations for pressure and fragment perforation calculation. The proposed model consists of two sub-models: a crevasse damage sub-model and a shock damage severity sub-model. The former utilizes a fifth-order analytic hierarchy process structural model, while the latter utilizes the fuzzy theory. Combining the two sub-models yields the total survivability of the propulsion system of a naval ship. The model is applied to assess the survivability of three propulsion system design types (CODOG, CODAD, and CODAG) for a 3000 T class frigate. Results demonstrate the utility of the proposed model as a fast and robust method for use during iterative design cycles, enabling design changes based on the analysis results.

Key words: *Fuzzy theory; Ship survivability; Propulsion system; Analytic hierarchy process; Shock environment*

1. Introduction

In his famous book titled Discussion of Questions in Naval Tactics [1], Stepan O. Makarov, a highly accomplished and decorated commander of Imperial Russian Navy, pointed out, maybe for the first time, that: "…the most important task of a naval ship designer is to qualify the operational capability and survivability of a warship in a battlefield environment…" The survivability of a warship can be divided into susceptibility, vulnerability, and recoverability, according to the standards of the Office of the Chief of Naval Operations (OPNAV) [2]. According to the history of warship development, the vulnerability assessment has always played a very important role in identifying the level of operational capability that must remain after damages had been induced by anti-ship weapons, such as mines, torpedoes, and cruise missiles [3-6].

A close analysis of warship system survivability from actual combat and target practice is severely limited due to military reasons. The studies mentioned above have primarily focused on the pure theory of survivability, ultimate strength problems of damaged ship structures, and large-scale experimental investigations. Jolliff provided viewpoints on navy ship survivability and concludes that the navy and industry must work together on established goals to achieve a high level of survivability [7]. In 1990, the U.S. Navy selected a layered hardening approach to the electromagnetic pulse survivability of mission-critical systems of surface ships; the approach consists of platform-level hardening and system-level hardening [8]. Ball and Calvano proposed a conceptual structure of ship survivability definitions and concepts and emphasized the need to incorporate a total-ship approach to surface naval ship survivability into ship design philosophy [9]. Naval ships are multifunctional, fulfilling front-line roles and routine operations, such as continuous surveillance and humanitarian assistance, to maximize return on investment for their owners. Thus, the necessity of survivability design technique on Korean naval vessels and the guidance on its development are discussed in [10]. Primorac and Parunov developed a probabilistic model of reduction in the bending moment capacity of an oil tanker following grounding and collision accidents; the authors used the Monte Carlo (MC) simulation with the probability distributions of damage parameters [11]. Vladimir *et al*. presented a procedure for strength assessment of a partially grounded ship structure in mud, which can be used to determine the reaction pressures of sunken ships in salvaging operations and similar problems of sunken vessels [12]. The impact resistance of a stringer-stiffened panel subjected to blunt impact loading is studied by Kubit *et al.* [13]. To reveal the impact stability characteristics of thin-walled C-cross section beams subjected to dynamic axial forces, FEM calculations and experimental tests are given by Mališ and Šimić Penava [14]. The results show that both global and local buckling failures are common occurrences. Vrgoč, Tomićević, Zaplatić *et al*. presented experimental studies to observe the damage initiation and growth in a glass fibre reinforced epoxy resin composite by using the FE-based digital image corelation technology [15].

Apart from total ship survivability assessment (TSSA) methods, a new reliable method named volumetric integrated vulnerability assessment methodology was recommended by the U.S. Naval Sea Systems Command (NAVSEA) for surface combatants and amphibious warfare ships to assess the vulnerability performance of multiple concept level ship design [16]. In the study [17], new metrics for the survivability and continuity of service were proposed; they enable a better definition of power system requirements related to the operational needs of a naval ship. Piperakis pointed out that some survivability assessment tools currently exist [18]; however, most fail to integrate all survivability constituents (susceptibility, vulnerability, and recoverability) in that they are unable to balance between the component features of survivability. In their study, Kim, Hwang, and Li described the ship vulnerability after a penetration hit and incorporated a vulnerable area approach to the naval ship survivability; they used the kill tree method, Markov chain method, and Poisson method in the case of multiple hits on the critical components [19]. To clarify different survivability measures, Liwång and Jonsson examined the sensitivity of the calculated probabilities to changes in the threat description; their analysis shows that the threat must be treated as uncertainty, which also should be reflected in the output and weighted in the decisions made [20]. In his next study, based on the Bayesian network and uncertainty Monte Carlo analysis, Li-wang shows that it is possible to link the performance of specific ship design features to the operational risk [21].

Wright revisited the legacy of WWII vulnerability and applied it to modern warship design; this study reminds us of the biases of current practices and considers what has been lost but can be re-learned [22]. The probabilistic methodology is adopted in the warship context considering and defining the survivability characteristics of a ship in a preliminary design step [23]. The ship fire survivability is described and investigated based on a risk-based approach that can link the probabilistic survivability theory and survivability measure selection. This

analysis shows that the reliability and validity of identifying potential fires depend on the qualitative and outward-focused analysis of the ship's intended operation [24]. Reference [25] provides a simplified preliminary vulnerability modelling approach and an analysis tool for exploring the naval ship system vulnerability, while the software developed by the Krylov State Research Centre enables quantitative survivability assessments of surface ships and submarines with a long-history simulation [26]. The effects of structural protection on ship survivability are also analysed through a statistical computer-based simulation of an 8000T ship hit by a weapon with a 150 kg TNT charge warhead [27]. Most existing vulnerability models assess the vulnerability of pre-defined concepts and focus on systems rather than capabilities. To address this limitation, a new method based on a discrete Markov chain and associated transition matrix for assessing the vulnerability of distributed systems in the concept phase is proposed in [28]. This approach not only evaluates the vulnerability of a pre-defined concept but also provides directions for finding other, potentially superior solutions. Furthermore, a novel adaptable network-based approach is utilized to develop a vulnerability assessment method in the early-stage design, which reduces the design fidelity required for modelling and simulation. Based on the data obtained from experts, Hoang [29] presented a novel analytic hierarchy process (AHP) for estimating risks of ship systems. After that study, Hoang introduced a new similarity/dissimilarity measure for intuitionistic fuzzy sets for pattern recognition applications [30]. In order to calculate vibration of the ship propulsion system under excitation, new analytical procedures for the vibration analysis of the ship shafting system are presented in [31-32]. By using the multiple criteria decision-making AHP model, Krstic, Gvozdenovic, and Mirosavljevic wrote a methodology for evaluating the safety level of aircraft performance [33].

The survivability assessment of naval ship propulsion systems can be significantly affected by weapons or human factors; however, their influence on the assessment process cannot be determined with certainty. To address this issue, a model based on the fuzzy theory and the AHP is developed to analyse such systems. The present model is based on the classification and summary of damage effects, derived from semi-empirical formulations or finite element method (FEM) simulations of propulsion systems of a general frigate or a destroyer. A fifth-order AHP structural model and the fuzzy theory are used to build both crevasse damage sub-models and shock damage severity sub-models for the vulnerability step. The fuzzy analysis process considers several fuzzy effects, including crevasse damage severity, shock damage severity, and other non-qualitative factors, using exponential-type membership function descriptions. By normalizing different fuzzy damage matrices, the vulnerability of propulsion system components, such as gas turbines, synchro clutches, and gearbox, is obtained. As a practical example, the survivability of three propulsion system designs (CODOG, CODAD, and CODAG) for a 3000T class frigate is assessed. The results demonstrate that the proposed model based on the fuzzy theory and AHP provides a reasonable prediction for the concept design process of the 3000T class frigate propulsion system. These results enable iterative design cycles based on the analysis results provided by the model.

2. The weapon damage effects on the naval ship propulsion system

2.1 The types of naval ship propulsion systems

Naval propulsion systems typically consist of machinery, equipment, and controls that are mechanically, electrically, or hydraulically connected to a propulsion shaft. In nearly all naval ships, a screw-type propeller is utilized as the propulsion device. A schematic of typical surface vessel's propulsion plants is shown in Figure 1, with its primary components discussed in detail below.

The thrust generated on the propeller is transmitted to the ship's structure through the main shaft via the thrust bearing (Fig. 2). The main shaft runs from the reduction gear main

shaft to the propeller and is supported and maintained in alignment by spring bearings, stern tube bearings, and strut bearings. The thrust on the propulsion shaft, generated from the pushing effect of the propeller, is transmitted to the ship's structure through the main thrust bearing. The majority of naval ships have the main thrust bearing situated at the front end of the main shaft within the main reduction gear casing. However, in some larger naval ships, the thrust bearing of the main shaft is situated further aft in the machinery space or the shaft alley. The main reduction gear connects the prime mover, or engine, to the shaft. The primary function of the main reduction gear is to decrease the high rotational speeds of the engine, allowing for the propeller to operate at lower rotational speeds. This mechanism enables both the engine and the propeller shaft to rotate at their most efficient speeds.

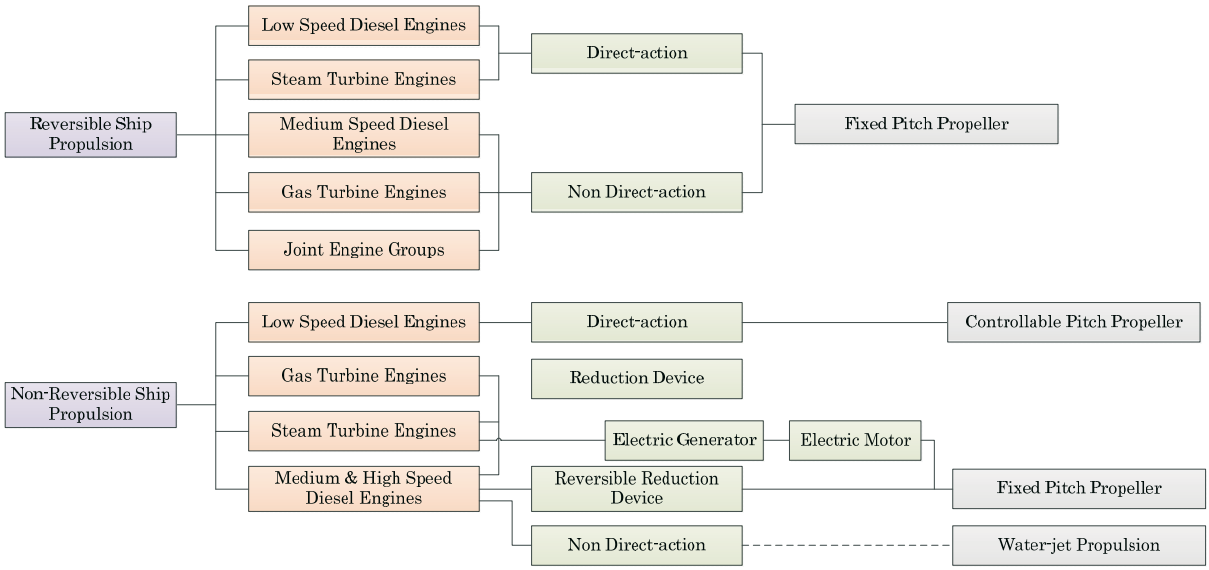

Fig. 1 Classification table of the propulsion architecture of a typical naval ship

The general ship propulsion architecture is based on the power required, the duty cycle, environmental concerns, and many other factors. Some of the most popular cycles used for naval ship propulsion employing the GE and Rolls-Royce Marine gas turbines are:

(1) Combined gas turbine system and mechanical drive propellers (COGAG);
(2) Combined gas turbine and diesel mechanical drive (CODAG);
(3) Combined gas turbine or diesel mechanical drive (CODOG);
(4) Hybrid drive options: combined diesel electric or gas turbine (CODOG);
(5) Integrated electric propulsion combined gas turbine and/or diesel electric.

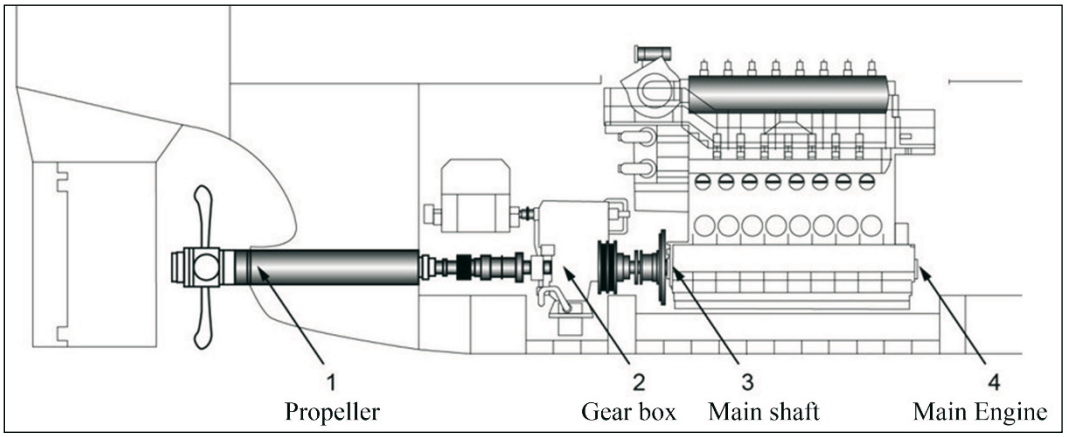

Fig. 2 Illustration of a typical ship propulsion system

The well-proven LM2500 aeroderivative gas turbine produced by GE has been directly derived from the GE CF6 family of commercial aircraft engines and GE TF39 military engines. Each DDG-51 ship is powered by four LM2500 gas turbines which are in a combined gas and gas (COGAG) configuration. The LM2500 was again uprated in 1993 for use on the US Navy's newest Sealift gas turbine-powered ships. The type 42s guided missile destroyer did not have the missile Ikara and the obsolete Limbo ASW mortar, while the COSAG (combined steam and gas) propulsion plant was replaced with a COGOG (combined gas turbine or gas turbine) one. Power was generated by a COGOG arrangement which contained two Rolls-Royce 'Olympus' TM3B high-speed gas turbines coupled with two Rolls-Royce 'Tyne' RM1C gas turbines, producing 50,000 horsepower and 5,340 horsepower, respectively. The combined gas turbine or diesel mechanical drive (CODOG) types were also used in some frigates; for example, the ROKS Cheonan (PCC-772) [34], a Pohang-class corvette (a small, manoeuvrable and armed warship), served as part of the South Korean Republic of Korea Navy (Fig. 3).

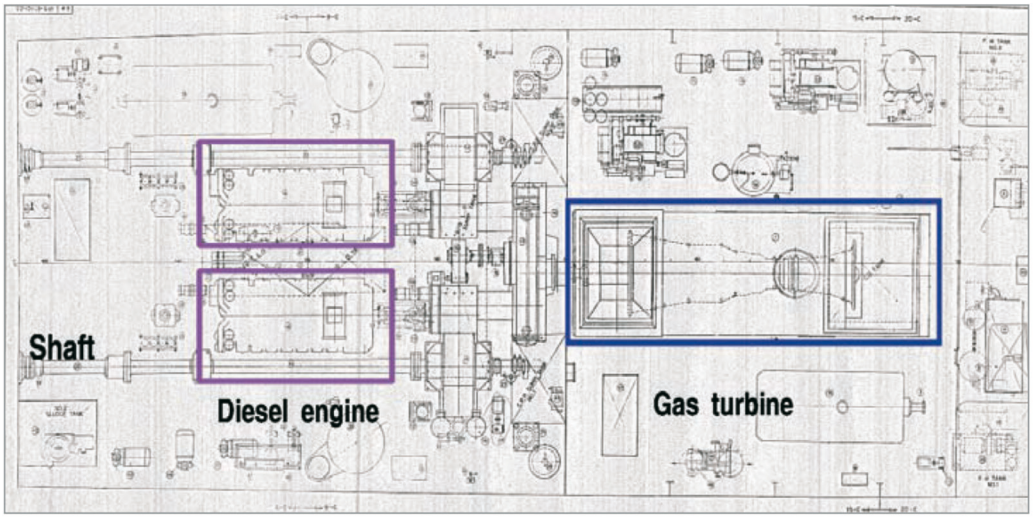

Fig. 3 A gas turbine and diesel engines (CODOG) installed on ROKS Cheonan, South Korea

2.2 Damage characteristics in severe shock environments

The damage failure mechanism of a naval vessel's propulsion system is very complex. The studies [35–36] reveal that the dynamic response of equipment (such as a supercharging boiler) changes with water depth and attack angle. In the combat environment, the anti-ship weapons can be traditionally categorized into four types: mines, torpedoes, bombs, and anti-vessel missiles. A naval mine is a self-contained explosive device placed in water to damage or destroy surface ships. The damage caused by a mine depends on the initial power of the explosion, and the distance between the target and the detonation, which can be described as a shock factor [37].

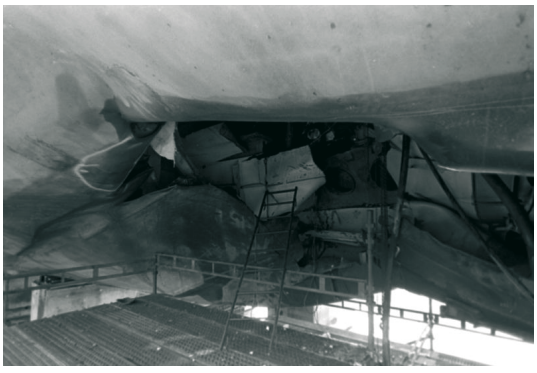
Damage to USS Samuel B. Roberts caused by a mine

Damage to USS Independence caused by a torpedo

Fig. 4 The characteristics of damage to ships caused by a mine and a torpedo

As the second weapon type, the modern torpedo is a self-propelled streamline weapon with an explosive warhead, launched above or below water surface, propelled underwater towards a target, and designed to detonate either on contact with its target or in proximity to it. One of the significant advantages of the modern torpedo is its low noise and long self-guidance operating distance, which make it a stealthy weapon. The torpedo inflicts damage to the target similar to that of a mine, but there are some differences. Specifically, the damage area and crevasse area caused by a naval mine are larger than those caused by a torpedo. Furthermore, the crevasse depth caused by a naval mine is less than that caused by a torpedo. The steel plate crevasse caused by a naval mine is usually turned toward the inside, while the steel plate crevasse caused by a torpedo can be turned either toward the inside or outside. The damage characteristics of United States Ship (USS) Samuel B. Roberts (FFG-58) and USS Independence (CVL-22) are shown in Fig. 4 [38-39].

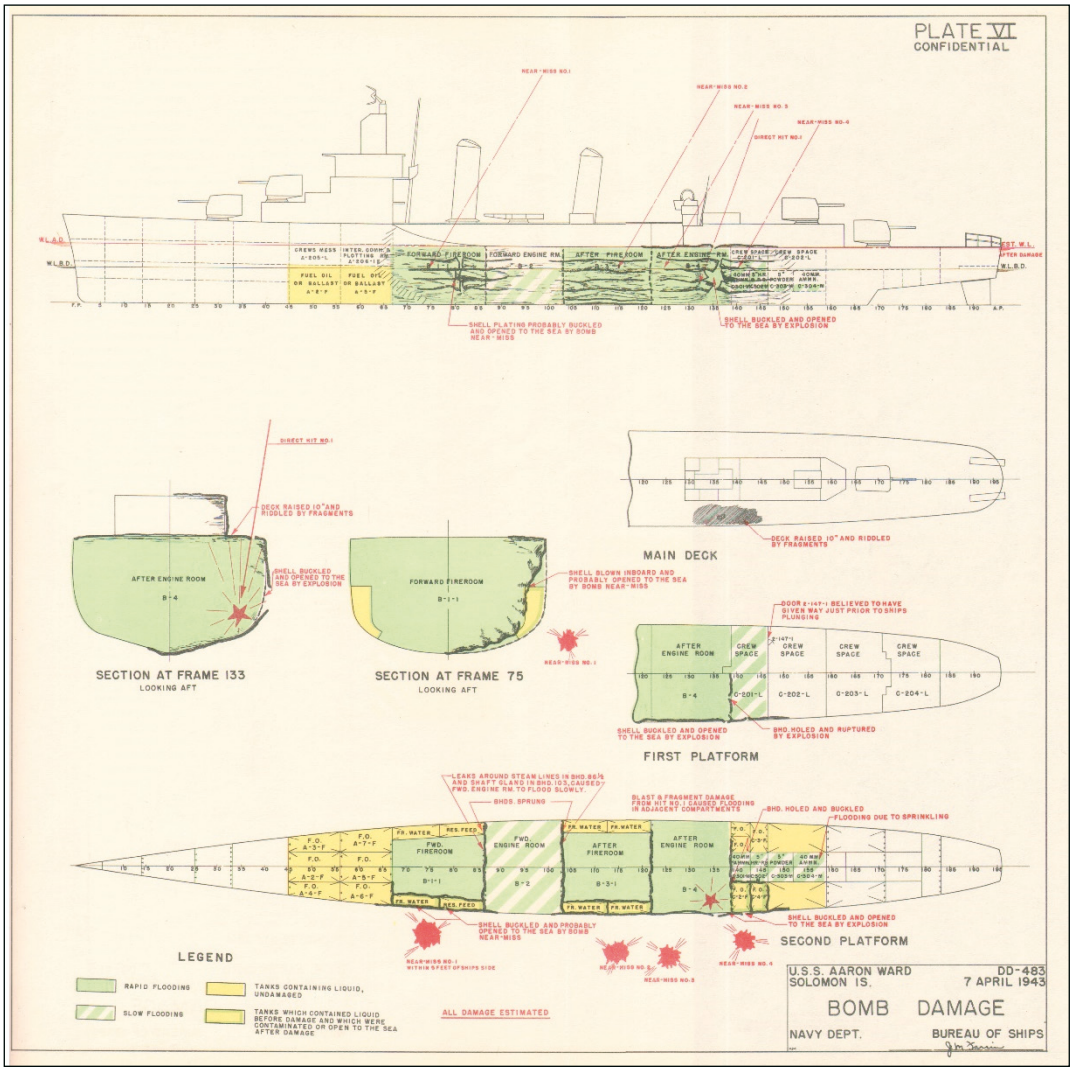

Fig. 5 USS MAYRANT (DD402) near-miss bomb damage [36]

The third cause of damage in naval warfare encompasses aerial bombs and shipboard-gun bombs, while a significant cause of damage lies in suicide aircraft, which share characteristics with aerial bombs. Typically, bombs are categorized as either explosive, armour-piercing, or semi-armour-piercing. Explosive bombs produce a non-contact air or underwater explosion (UNDEX) shock wave. In contrast, armour-piercing and semi-armour-piercing bombs penetrate the ship panel before exploding within the compartment, resulting in an air blast shock wave, fragment penetration, and fire damage. A depiction of the near-miss bomb damage inflicted to USS MAYRANT (DD402) is shown in Fig. 5 [40].

The last, but the most serious threat to modern warships may be the anti-ship missile. The first anti-ship missile, the SS-N-2 Styx (P-15Termit) missile, was used in the Middle East. In 1967, the Israeli destroyer Eilat was the first ship to be sunk by a ship-launched missile (some Styx missiles launched by Egyptian Komar-class missile boats off the Sinai Peninsula). There are several types of anti-ship missiles, such as blast warhead (BW), shaped-charge warhead (SCW), and semi-armour-piercing warhead (SAPW). Despite the variety of anti-ship missiles, the basic damage inflicted by an anti-ship missile is similar to that inflicted by a torpedo, excluding underwater penetration. As the history of the anti-ship missile is short, the number of available actual combat and target practice examples is limited. A typical damage inflicted to HMS Sheffield by an anti-ship missile attack is shown in Fig. 6 [41].

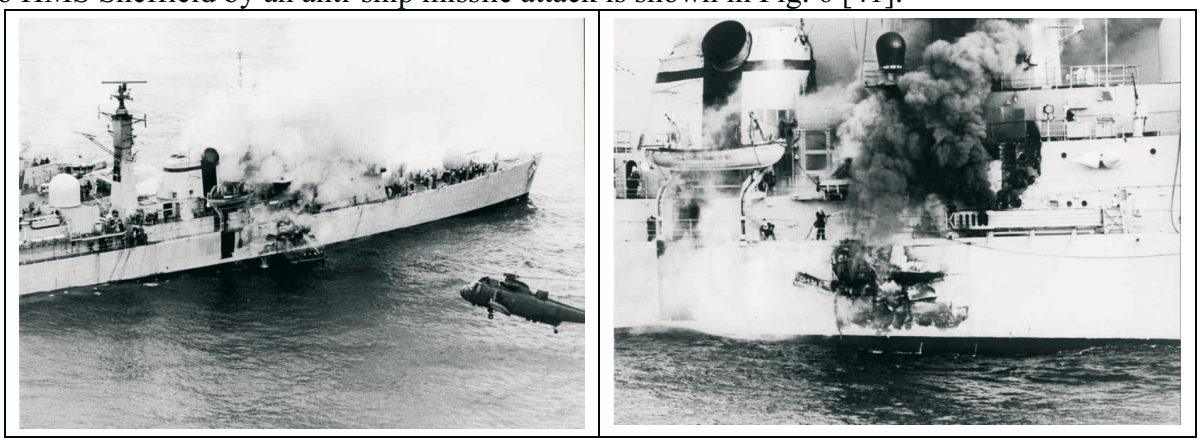

Fig. 6 The damage to HMS Sheffield caused by the attack of Exocet missile [41]

Due to the complexity of practical cases, conventional weapons always contain one, two or more damage effects. Based on the damage characteristics of four conventional anti-ship weapons, nine types of effects of four weapons are summarized and shown in Fig. 7. To simplify the damage process, the main four damage forms including the explosion-caused fire-induced damage, high-speed fragment penetration-induced damage, high-level shock acceleration damage caused by a wave, and the flooding of power room caused by an out-off hull crack, are considered in the present study (Fig. 7).

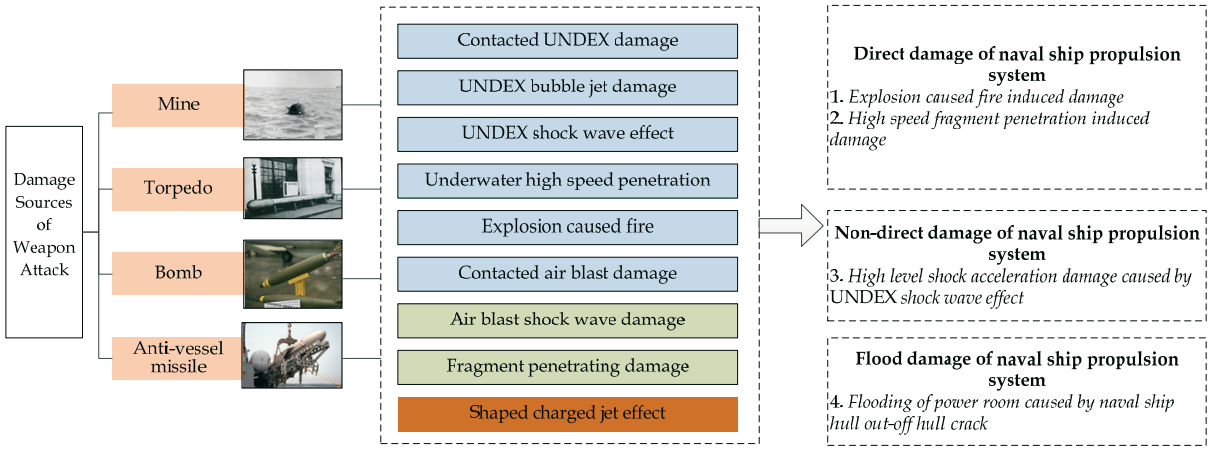

Fig. 7 The damage effects of four weapons (The figure has been taken from google pictures)

2.2.1 Direct damage type

The direct damage to the naval ship propulsion system is generally caused by explosion fire and high-speed fragments. To determine whether the propulsion system equipment is damaged or not, the critical point is to establish relationships between the damage criterion and

stand-off distance (the distance between weapon explosive charge points and equipment). Firstly, the distance l is obtained by the following expression:

$$l = \sqrt{(X_g - X)^2 + (Y_g - Y)^2 + (Z_g - Z)^2}\ , \tag{1}$$

where X, Y, Z are the coordinates of the power system equipment in the x, y, z directions, respectively; X_g, Y_g, Z_g are the coordinates of weapon explosive charge points in the x, y, z directions, respectively.

For the first direct damage type, named fire-induced damage caused by explosion, the description of the explosion fire is simplified as a spherical ball. The diameter and the length of time, i.e., duration of a spherical ball, are given as in [42]:

$$D_f = 3.86 M_e^{0.320}, \quad T_f = 0.299 M_e^{0.320}, \tag{2}$$

where D_f is the diameter of a fire spherical ball caused by explosion, T_f is the duration of a fire spherical ball caused by explosion, and M_e is the mass of explosive charge. If the distance l is smaller than the diameter D_f, the damage will occur.

For the second direct damage type, named damage induced by high-speed fragment penetration, the distribution of fragment speed can be assumed as a uniform distribution. If the total number of high-speed fragments is set as N, the number n, which refers to the number of fragments that is hitting the power equipment, is set as bellow [42]:

$$n = \frac{N}{4\pi l^2} S \tag{3}$$

$$S = LH\cos\alpha\cos\beta + LB\sin\beta + BH\sin\alpha \tag{4}$$

$$\alpha = \operatorname{arctg}\frac{Y_g - Y}{Z_g - Z} \tag{5}$$

$$\beta = \operatorname{arctg}\frac{Z_g - Z}{X_g - X}, \tag{6}$$

where S is the exposure area, L, B, and H are the length, breadth, and height of power equipment, and l is the stand-off distance; α and $\beta$are the angles. Thus, we introduce the efficient area coefficient K, expressed as

$$K = \frac{Damage\ \ Area\ \ of\ \ Power\ \ Equipment}{Exposure\ \ Area\ \ of\ \ Power\ \ Equipment}, \tag{7}$$

and the efficient number of high-speed fragments, expressed as

$$M = \frac{N}{4\pi l^2} KS\,. \tag{8}$$

2.2.2 Non-direct damage type

The non-direct damage to propulsion system is usually caused by a shock transmission process. The high-level shock acceleration damage is its main characteristic; its damage ratio can be estimated by the following expressions [42]:

$$R_z = \frac{\mu\kappa M_e^{2/3}}{\sigma t}\sqrt{\frac{E}{\rho}}\ , \quad \mu = 1.93, \quad \kappa = 50.0 - 60.0\,, \tag{9}$$

where R_z is the damage ratio, M_e is the mass of the explosive charge, σ is the yield stress of the base material, t is the thickness of the ship shell structure, k is the explosive parameter, μ is the structure parameter, E is the modulus of elasticity of the base material, and ρ is the density of the base material.

Another simple criterion to calculate the non-direct damage to a propulsion system is adopting a critical damage acceleration [42],

$$A_{x(y,z)}=\begin{cases}\geq A'_{x(y,z)}, & damage\\ < A'_{x(y,z)}, & not\ damage\end{cases}, \tag{10}$$

where $A_{x(y,z)}$ is the shock acceleration in the x (y, z) direction, and $A'_{x(y,z)}$ is the critical damage acceleration in the x (y, z) direction. The critical damage acceleration, $A'_{x(y,z)}$, can be obtained by the anti-shock finite element analysis (FEA) or the empirical formulae from experiments.

2.2.3 Flood damage type

The third damage type, named flood damage to naval ship propulsion system, is the most serious damage type caused by crevasse. The dimensions of a crevasse are estimated by the following empirical formula [43-44]:

$$R_p=0.0704\sqrt{\frac{M_e}{t}} \tag{11}$$

or

$$2R_p=0.063\frac{\sqrt{M_e}}{\sqrt[3]{t}\cdot I'^{0.153}}, \tag{12}$$

where M_e is the mass of explosive charge, t is the equivalent thickness of the ship's stiffened structures, and I' is the equivalent thickness of the ship's stiffened structures.

3. The evaluation of the mathematical model

3.1 A model for the assessment of a direct or a flood damage, based on the fuzzy theory and AHP

To simplify the analysis, the direct damage to the propulsion system of a naval ship is classified into four types, i.e., the damage caused by the low-capacity weapons, medium-capacity weapons, high-capacity weapons, and nuclear weapons [45]; the classification of weapons and examples are given below:

M_1—low-capacity weapons; for example, guns, high-explosive charges, and penetration charges;

M_2—medium-capacity weapons; for example, sea-skimming missiles, torpedoes, and mines;

M_3—high-capacity weapons; for example, high-energy guns and near-explosion missiles;

M_4—nuclear weapons.

The general types of attacks, classified into four types, are given below:

N_1—underwater direct hitting on the naval ship port side;

N_2—underwater direct hitting on the naval ship starboard;

N_3—direct-hitting on the naval ship in the air;

N_4—nuclear weapon explosions out of a safe distance.

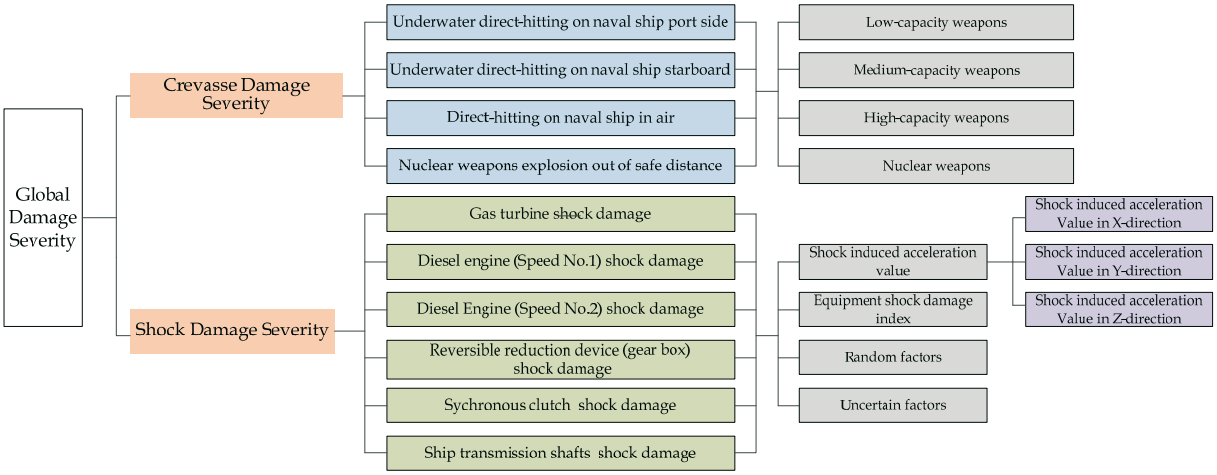

Fig. 8 A fifth-order analytic hierarchy process (AHP) structural tree model

For a frigate or a classic destroyer (like a Spruance-class destroyer), generally, B/L_{OA}<0.1, where B is the ship breadth, and L_{OA} is the length over all. For modern destroyers, such as Arleigh Burke-class destroyers, B/L_{OA}~0.125. However, for some large vessels like aircraft carriers, e.g., Gerald R. Ford-class aircraft carriers, B/L_{OA}~0.2. In our analysis, if B/L_{OA}<0.15, we assume that the third attack type direct-hitting on the naval ship in the air is indifferent to the left-right divide. On the other hand, if B/L_{OA}<0.15, the clear direction of the third attack type direct-hitting in the air must be divided. The damage scope of the first and second attack types can be calculated by Eqs. (1)-(6) or Eqs. (3)-(10), and the hitting probability distribution is set as uniform. If the damage scope incorporates the power room, the shaft power is lost. If the underwater direct-hitting occurs near the left(right) shaft, the shaft will be damaged. The shaft will be safe if direct-hitting on the naval ship is in the air. For the last attack type, the nuclear weapon explosion out of a safe distance, the damage to room structures and equipment is set as random distribution. Three important elements of the fuzzy theory and AHP are: a set of factors, an alternative set, and single factor assessment. Thus, for our assessment scope, they include the following: a two-factor set list, such as the assessment object set **U**, which includes a weapon type set and an attack type set,

$$\mathbf{M} = \left(M_1, M_2, ...M_i\right), i = 1 \sim 4, \tag{13}$$

a general attack type set,

$$\mathbf{N} = \left(N_1, N_2, ...N_j\right), j = 1 \sim 4, \text{ and} \tag{14}$$

an assessment language set **V**,

$$\mathbf{H} = (h_1, h_2, ...h_k), k = 1, 2...., \tag{15}$$

where **H** is the damage severity grade of the system, and h_k is the power loss percentage; its value is based on the general arrangement and the weapon damage effect. As for three space dimensions, the damage function can be described as $f(M_i, N_j, h_k)$.

The fuzzy matrix of a power system under different weapons R is expressed as the fuzzy relation between the assessment object set **U** and the assessment language set **V**,

$$\mathbf{U} \xrightarrow{R} \mathbf{V}. \tag{16}$$

The fuzzy matrix of weapon threat to the power system is set as

$$\boldsymbol{\omega} = (\omega_1, \omega_2, ...\omega_j) \tag{17}$$

$$\mathbf{F} = \begin{pmatrix} F_1 \\ \vdots \\ F_j \end{pmatrix}_{j \times k} = f \cdot R. \tag{18}$$

Thus, the assessment matrix **F** can be obtained. The probability of damage is expressed as

$$\mathbf{P} = \boldsymbol{\omega} \cdot \mathbf{F} = (P_1, P_2, ...P_k) \tag{19}$$

$$\mathbf{S}_1 = \mathbf{P} \cdot \mathbf{H}^T. \tag{20}$$

3.2 A model for shock damage assessment, based on the fuzzy theory and AHP

The assessment of shock damage to mechanical or electrical equipment is a complex task that involves a number of uncertain and fuzzy factors, such as the lack of uniformity in shock damage assessment standards. The study [45] predominantly relied on the acceleration criteria or shock response spectrum analysis for evaluation purposes. However, it should be noted that the extent of shock damage is intricately linked to a range of variables, including the nature of the explosion source, duration of the shock, and structural characteristics, among others. Here, a fuzzy theory-based model has been developed; the model takes into account three installation types: single-stage shock isolation, two-stage shock isolation, and direct rigid shock isolation.

For shock damage severity, the assessment language set can be described as

$$\mathbf{V} = (V_1, V_2, V_3, V_4, V_5), \tag{21}$$

where V_1 indicates that the propulsion system is well, V_2 indicates the minor damage to the naval propulsion system, V_3 indicates the medium damage to the naval propulsion system, V_4 indicates the serious damage to the naval propulsion system, and V_5 indicates the complete loss of the naval propulsion system. The corresponding damage matrix is given as

$$\mathbf{H} = (h_1, h_2, h_3, h_4, h_5) = (0, 0.25, 0.5, 0.75, 1.0), \tag{22}$$

where h_i=(i=1, 2, …5) are the weight coefficients.

The assessment object set **U** can also be divided into three hierarchical processes;

$$\mathbf{U}_1 = (U_{11}, U_{12}, U_{13}, U_{14}, U_{15}, U_{16}), \tag{23}$$

where U_{11} is the gas turbine, U_{12} is the diesel engine with a single-stage shock isolator, U_{13} is the diesel engine with a double-stage shock isolator, U_{14} is the diesel engine with a double-stage shock isolator, U_{15} is the synchronous clutch, and U_{16} is the bearing of shafts;

$$\mathbf{U}_2 = (U_{21}, U_{22}, U_{23}, U_{24}), \tag{24}$$

where U_{21} is the shock damage indicator K, U_{22} is the shock response value, U_{23} is the measurement of non-quantitative factors such as stand-off distance or explosion cause, U_{24} is the measurement of some random factors;

$$\mathbf{U}_3 = (U_{31}, U_{32}, U_{33}, U_{34}), \tag{25}$$

where U_{31} is the vertical acceleration in the Z-direction, U_{32} is the acceleration in the Y-direction, U_{33} is the acceleration in the X-direction, and U_{34} is the initial velocity. All the factors

in the sets, except for U_{23} and U_{24}, can be analysed quantitatively by adopting the expression for the fuzzy membership function, while U_{23} and U_{24} are evaluated by fuzzy statistics or the expert's judgement. The fuzzy membership function with normal distribution types is given as

$$\mu_{vi}(x) = e^{-\left(\frac{x-a}{b}\right)^2},\ i = 1,2,\cdots 5. \tag{26}$$

The basic characteristics of $\mu_{vi}(x)$ are summarized as follows: firstly, the membership grade of $x \in \{x<x_1\} \cup \{x>x_5\}$ is 1; if $x \in \{x>x_5\}$, the membership grade of the mid-point range is 1; secondly, the membership grade of the cross point of adjacent region is 0.5. According to the above two rules, the values of coefficients a and b in the membership function can be obtained; they are given in Table 1 and Table 2. Each factor is expressed as

$$r_{ij} = \mu_{vi}(x) = e^{-\left(\frac{x_i - a_j}{b_{ij}}\right)^2} (i = 1\cdots 5, j = 1\cdots 5), \tag{27}$$

and the first layer fuzzy matrix is given by

$$\mathbf{R} = \left(r_{ij}\right)_{i\times j}. \tag{28}$$

Thus, the shock damage severity $\mathbf{S}_2$ can be obtained by a fuzzy comprehensive assessment.

Table 1 Factor range values of shock damage severity

	Shock damage severity	V_1	V_2	V_3	V_4	V_5
K	(x_i, x_{i+1}), i=1,2…5	0	[0, 0.3]	[0.3, 0.6]	[0.0, 1.0]	1.0
	Mid-point	0	0.15	0.45	0.8	1.0
a_V (g)	(x_i, x_{i+1}), i=1,2…5	[0, 120]	[120, 160]	[100, 200]	[200, 400]	[240, 280]
	Mid-point	60	140	180	220	260
a_B (g)	(x_i, x_{i+1}), i=1,2…5	[0, 70]	[70, 100]	[100, 120]	[120, 150]	[150, 190]
	Mid-point	35	85	110	135	170
a_L (g)	(x_i, x_{i+1}), i=1,2…5	[0, 50]	[50, 70]	[70, 90]	[90, 110]	[110, 140]
	Mid-point	25	60	80	100	125
V(m/s)	(x_i, x_{i+1}), i=1,2…5	[0, 2.5]	[2.5, 3.0]	[3.0, 4.0]	[4.0, 5.0]	[5.0, 6.0]
	Mid-point	1.25	2.75	3.5	4.5	5.5

Table 2 Values of coefficients a and b

Severity factor	K		a_V		a_B		a_L		V	
	a	b	a	b	a	b	a	b	a	b
V_1	0	0	60	72	35	42	25	30	1.25	1.5
V_2	0.15	0.18	140	24	85	18	65	12	2.75	0.3
V_3	0.45	0.18	180	24	110	18	85	12	3.5	0.6
V_4	0.8	0.24	220	24	135	18	110	12	4.5	0.6
V_5	1	0	260	24	170	24	125	18	5.5	0.6

Thus, the shock damage severity $\mathbf{S_2}$ can be obtained by a fuzzy comprehensive assessment. Based on the damage severities $\mathbf{S}_1$ and $\mathbf{S}_2$ calculated in sections 3.1 and 3.2, the survivability of the propulsion system AM is

$$AM = 1 - S, \tag{29}$$

$$S = \omega_1 S_1 + \omega_2 S_2 \tag{30}$$

4. Practical example assessment: propulsion system of a 3000 T class frigate

4.1 The design of the propulsion system

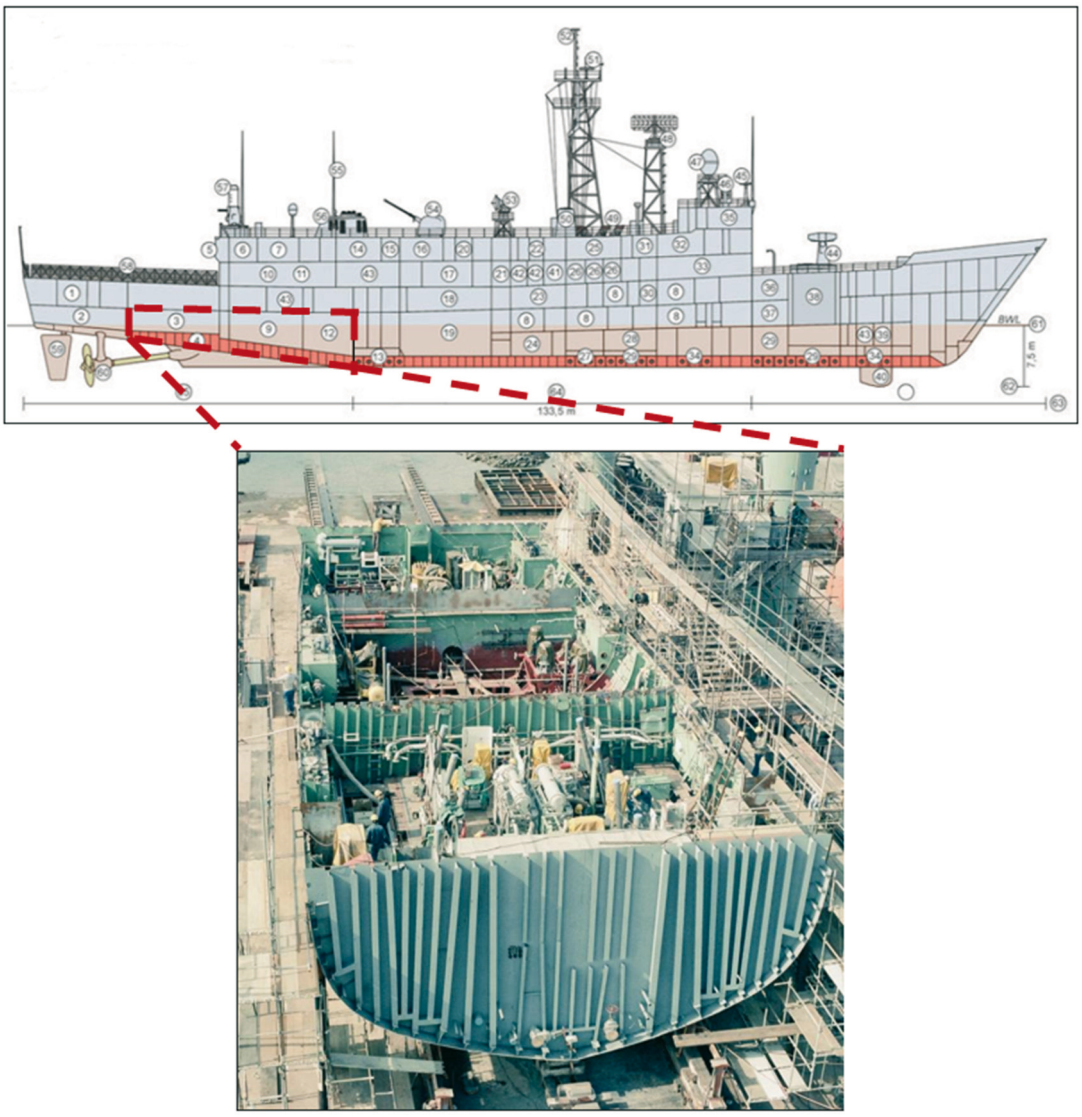

Fig. 9 General arrangement of the propulsion system of an *Oliver Hazard Perry-class* frigate [46]

As a practical example, the survivability of three propulsion system design types (CODOG, CODAD, and CODAG) for a 3000 T class frigate as a simplified example of an ***Oliver Hazard Perry-class*** frigate, is evaluated [46] (Fig. 9). The main parameters of these three designs are given in Table 3.

Table 3 Main parameters of CODAD, CODOG and CODAG for a 3000 T class frigate

Parameters	CODAD	CODOG	CODAG
Type of diesel engine	PA6-STC-16	MTU 20V-1163-TB93	MTU-20V-1163-TB82
Power of diesel engine	4*7050HP	2*7510HP	2*5500HP
Type of gas turbine	-	LM2500-30	LM2500-30
Power of gas turbine	-	1*30400HP	1*30400HP
Division number of main engine room	3	3	2
Length of forward main engine room L_F	9.5 m	10.5 m	14.5 m

Length of afterward main engine room L_B	10.5 m	9.5 m	8.0 m
Length of gear box room L_C	5.5 m	5.5 m	-
Distance between afterward main engine bulkhead and propeller L_P	35.0 m	48.2 m	47.0 m
Water length L	120 m	120 m	120 m
Types of vibration isolator of gas turbine	-	Single layer vibration isolation	Single layer vibration isolation
Types of vibration isolator of diesel engine at service speed	Double layer vibration isolation	Double layer vibration isolation	Single layer vibration isolation
Types of vibration isolator of diesel engine at acceleration speed	Single layer vibration isolation	-	-
Types of vibration isolator of gear box	Rigid mounting	Rigid mounting	Rigid mounting

4.2 The direct damage or flood damage assessment

According to the assessment model and the possible damage types listed in Fig. 7 and Fig. 8, the assessment matrix of direct or flood damage to the propulsion system is given in Table 4.

The damage hole diameter R can be evaluated from empirical formulae such as Eqs. (1)-(12) or numerical simulations. Practical combat statistical results show that the largest allowed damage hole diameters for different ships differ. For example, for a minesweeper or submarine chaser, it is about 2.0 m; for a frigate, it is about 2.0 m - 3.0 m; for a destroyer, it is about 3.0 m - 4.0 m; for a light cruiser, it is about 6.0 m - 8.0 m; and for a heavy cruiser, it is about 6.0 m - 8.0 m. In the present study, the damage hole diameter R is set as 3.0 m.

Table 4 Assessment matrix of direct or flood damage to the propulsion system

U	$V= H=(h_1, h_2, h_3)$				**Weight**
N_j	$\mathbf{M_j}$	100% Power lost	50% Power lost	0% Power lost	
N_1	M_1	2R/L	$(L_F+ L_B+L_P)$/L	1-2R/L-$(L_F+L_B+ L_P)$/L	0.3
	M_2	2R/L	$(L_F+ L_B+L_P)$/L	1-2R/L-$(L_F+L_B+ L_P)$/L	0.7
	M_3	0	0	1	0
	M_4	0	0	1	0
N_2	M_1	2R/L	$(L_F+ L_B+L_P)$/L	1-2R/L-$(L_F+ L_B+L_P)$/L	0.3
	M_2	2R/L	$(L_F+ L_B+L_P)$/L	1-2R/L-$(L_F+ L_B+L_P)$/L	0.7
	M_3	0	0	1	0
	M_4	0	0	1	0
N_3	M_1	2R/L	$(L_F+ L_B)$/L	1-2R/L-$(L_F+ L_B)$/L	0.15
	M_2	2R/L	$(L_F+ L_B)$/L	1-2R/L-$(L_F+ L_B)$/L	0.35
	M_3	2R/L	$(L_F+ L_B)$/L	1-2R/L-$(L_F+ L_B)$/L	0.5
	M_4	0	0	1	0
N_4	M_1	0	0	1	0
	M_2	0	0	1	0
	M_3	0	0	1	0
	M_4	(2R + L_F+L_B+ L_P)/L	0	1-(2R + L_F+L_B+ L_P)/L	0

For N_1~N_4 in Eq. (14), the following expressions are valid:

$$N_1 = \begin{bmatrix} \frac{6}{120} & \frac{55}{120} & \frac{59}{120} \\ \frac{6}{120} & \frac{55}{120} & \frac{59}{120} \\ 0.00 & 0.00 & 1.00 \\ 0.00 & 0.00 & 1.00 \end{bmatrix}, \; r_{11} = \begin{bmatrix} 0.3 \\ 0.7 \\ 0.0 \\ 0.0 \end{bmatrix}, \; N_2 = \begin{bmatrix} \frac{6}{120} & \frac{55}{120} & \frac{59}{120} \\ \frac{6}{120} & \frac{55}{120} & \frac{59}{120} \\ 0.00 & 0.00 & 1.00 \\ 0.00 & 0.00 & 1.00 \end{bmatrix}, \; r_{21} = \begin{bmatrix} 0.3 \\ 0.7 \\ 0.0 \\ 0.0 \end{bmatrix} \tag{31.a}$$

$$N_3 = \begin{bmatrix} \frac{6}{120} & \frac{20}{120} & \frac{94}{120} \\ \frac{6}{120} & \frac{20}{120} & \frac{94}{120} \\ \frac{6}{120} & \frac{20}{120} & \frac{94}{120} \\ 0.00 & 0.00 & 1.00 \end{bmatrix}, \; r_{31} = \begin{bmatrix} 0.15 \\ 0.35 \\ 0.50 \\ 0.0 \end{bmatrix}, \; N_4 = \begin{bmatrix} 0.00 & 0.00 & 1.00 \\ 0.00 & 0.00 & 1.00 \\ 0.00 & 0.00 & 1.00 \\ \frac{61}{120} & 0.00 & \frac{59}{120} \end{bmatrix}, \; r_{41} = \begin{bmatrix} 0.00 \\ 0.00 \\ 0.00 \\ 1.00 \end{bmatrix} \tag{31.b}$$

According to the four attack weapon types, the global damage matrix is obtained as

$$\mathbf{F} = \begin{bmatrix} 0.0375 & 0.3000 & 0.4125 \\ 0.0875 & 0.7000 & 0.9625 \\ 0.0250 & 0.0833 & 0.3917 \\ 0.5083 & 0.0000 & 0.4917 \end{bmatrix}. \tag{32}$$

Considering the weight factor matrix as

$$\boldsymbol{\omega} = \begin{bmatrix} 0.2500 & 0.2500 & 0.1500 & 0.3500 \end{bmatrix}, \tag{33}$$

the global fuzzy assessment result is shown as

$$\mathbf{P} = \boldsymbol{\omega} \cdot \mathbf{F} = \begin{pmatrix} 0.2129 & 0.2625 & 0.5746 \end{pmatrix}. \tag{34}$$

Here, the evaluation level is explored as presented for the three types of propulsion,

$$\mathbf{H} = \begin{bmatrix} 1.0000 & 0.5000 & 0.0000 \end{bmatrix} \tag{35}$$

$$\begin{aligned} \mathbf{S}_{\text{CODAD,1}} &= \mathbf{P} \cdot \mathbf{H}^T = 0.3441 \\ \mathbf{S}_{\text{CODOG,1}} &= \mathbf{P} \cdot \mathbf{H}^T = 0.4101 \\ \mathbf{S}_{\text{CODAG,1}} &= \mathbf{P} \cdot \mathbf{H}^T = 0.4187 \end{aligned} \tag{36}$$

Based on the results presented above, it is evident that the extent of damage inflicted to the three propulsion system design types, namely CODOG, CODAD, and CODAG, varies significantly. Specifically, the damage inflicted to the CODAG propulsion system is found to be the greatest, while that inflicted to CODAD is significantly smaller than that inflicted to the other two propulsion system types. In addition to propulsion system types, the arrangement of the main engine bulkhead and the length of the engine room are identified as the primary factors that can mitigate the direct damage caused by underwater explosions. Notably, the effect of the arrangement of the main engine bulkhead is found to be more significant than the effect of the length of the engine room; this is evidenced by the results presented in Table 3.

4.3 The shock damage assessment

There are two methods to evaluate the damage to a propulsion system caused by a shock wave: the FEM analysis and empirical formulae from the underwater explosion (UNDEX) tests. Here, in the initial concept design, the second method is adopted. As the literature on the shock-induced damage is limited, we refer to some open reports, such as [45], and express the average critical values for ship structures as

$$a_V=200\ g,\ a_B=120\ g,\ a_L=80\ g,\ \tau=0.025\text{s},\ V=49.0\ \text{m/s}. \tag{37}$$

For a gas turbine, if a saucer shock absorption damper is used, the stiffness K is $1.19*10^5$ N/m, and the shock responses of the gas turbine are about 0.8%-1.2% of input excitation. Thus, we can obtain

$$a_{VT}=2.00\ g,\ a_{BT}=1.20\ g,\ a_{LT}=0.80\ g,\ V_T=0.49\ \text{m/s}. \tag{38}$$

Using empirical data, the shock responses of a diesel engine with single-layer vibration isolation (the stiffness $K=5.6*10^7$ N/m) are found to be about 50.0% of input excitation.

$$a_{VA}=100.0\ g,\ a_{BA}=60.0\ g,\ a_{LA}=40.0\ g,\ V_A=24.5\ \text{m/s} \tag{39}$$

Also from empirical data, the shock responses of a diesel engine with double-layer vibration isolation (the stiffness $K_1=5.60*10^7$ N/m, $K_2=5.31*10^7$ N/m) are found to be about 10.0% of input excitation.

$$a_{VD}=20.0\ g,\ a_{BD}=12.0\ g,\ a_{LD}=8.0\ g,\ V_D=4.90\ \text{m/s} \tag{40}$$

For a synchronous clutch, we assume that

$$a_{VL}=100.0\ g,\ a_{BL}=60.0\ g,\ a_{LL}=40.0\ g,\ V_L=24.5\ \text{m/s}. \tag{41}$$

For a gear box, we assume that

$$a_{VG}=100.0\ g,\ a_{BG}=60.0\ g,\ a_{LG}=40.0\ g,\ V_G=24.5\ \text{m/s}. \tag{42}$$

By submitting Eqs. (37)-(42) into (21)-(29), we can obtain the first fuzzy assessment matrix for a diesel engine with single layer vibration isolation as follows:

$$\mathbf{R_{1A}}=\begin{bmatrix}0.7344 & 0.0622 & 0.0000 & 0.0000 & 0.0000\\ 0.7017 & 0.1453 & 0.0000 & 0.0000 & 0.0000\\ 0.7788 & 0.0130 & 0.0000 & 0.0000 & 0.0000\\ 0.0000 & 0.0000 & 0.0000 & 0.0000 & 0.0000\end{bmatrix} \tag{43}$$

Then, normalizing the matrix, we obtain:

$$\mathbf{R_{1A}}=\begin{bmatrix}0.9219 & 0.0781 & 0.0000 & 0.0000 & 0.0000\\ 0.8285 & 0.1715 & 0.0000 & 0.0000 & 0.0000\\ 0.9836 & 0.0164 & 0.0000 & 0.0000 & 0.0000\\ 0.0000 & 0.0000 & 0.0000 & 0.0000 & 0.0000\end{bmatrix}, \tag{44}$$

and the weight factor arrow of the matrix is given as

$$\mathbf{W_{1A}}=\begin{bmatrix}0.35 & 0.20 & 0.10 & 0.35\end{bmatrix}. \tag{45}$$

According to the first level fuzzy assessment, we can obtain

$$\mathbf{A_{1A}} = \mathbf{W_{1A}}\mathbf{R_{1A}} = \begin{bmatrix} 0.5867 & 0.0633 & 0.00 & 0.00 & 0.00 \end{bmatrix}, \tag{46}$$

$$\mathbf{A_{2A}} = \begin{bmatrix} 0.0 & 0.0 & 0.15 & 0.84 & 0.00 \end{bmatrix}. \tag{47}$$

Referring to the literature for the weighting setting of unknown factors [47], the other assessment arrows are given as

$$\mathbf{A_{3A}} = \begin{bmatrix} 0.0 & 0.36 & 0.48 & 0.32 & 0.00 \end{bmatrix}, \tag{48}$$

$$\mathbf{A_{4A}} = \begin{bmatrix} 0.0 & 0.48 & 0.50 & 0.12 & 0.00 \end{bmatrix}. \tag{49}$$

The second fuzzy assessment matrix is expressed as

$$\mathbf{R_{2A}} = \begin{bmatrix} 0.5867 & 0.0633 & 0.0000 & 0.0000 & 0.0000 \\ 0.0000 & 0.0000 & 0.1500 & 0.8400 & 0.0000 \\ 0.0000 & 0.3600 & 0.4800 & 0.3200 & 0.0000 \\ 0.0000 & 0.4800 & 0.5000 & 0.1200 & 0.0000 \end{bmatrix}, \tag{50}$$

and its weight factor arrow is given as

$$\mathbf{W_{2A}} = \begin{bmatrix} 0.40 & 0.30 & 0.15 & 0.15 \end{bmatrix}. \tag{51}$$

Based on the second fuzzy assessment,

$$\mathbf{B_{1A}} = \mathbf{W_{2A}}\mathbf{R_{2A}} = \begin{bmatrix} 0.3610 & 0.1575 & 0.1825 & 0.3139 & 0.00 \end{bmatrix}. \tag{52}$$

The damage to a diesel engine with single layer vibration isolation is

$$\mathbf{S_A} = \mathbf{B_{2A}}\mathbf{H^T} = \begin{bmatrix} 0.3610 & 0.1575 & 0.1825 & 0.3139 & 0.00 \end{bmatrix} \begin{bmatrix} 0.00 \\ 0.25 \\ 0.50 \\ 0.75 \\ 1.00 \end{bmatrix} = 0.3661. \tag{53}$$

The damage evaluation results for the other equipment are shown in Table 5.

Table 5 Main parameters of three power system design types for a 3000T class frigate

Number	Equipment	CODOG
1	Gas turbine with single -layer vibration isolation	S_T=0.3562
2	Gas turbine with double-layer vibration isolation	S_D=0.3563
3	Synchronous clutch	S_L=0.4030
4	Gear box	S_G=0.5474
5	Bearing	S_B=0.5963

When the severity of damage to each part of the ship power system is obtained, using the assessment model from section 3.2, the shock survivability of each ship propulsion system is calculated as follows:

$$\begin{aligned} \mathbf{S}_{\text{CODAD,2}} &= 0.4337 \\ \mathbf{S}_{\text{CODOG,2}} &= 0.3932 \\ \mathbf{S}_{\text{CODAG,2}} &= 0.3966 \end{aligned} \tag{54.a}$$

The above calculation results show that the shock survivability of CODOG is better than those of CODAD and CODAG. This is mainly due to the double layer vibration isolator which can reduce the shock damage significantly, and it is more efficient than the single layer vibration isolator. Other reasons may be the arrangement of power system such as the division number of main engine room and the length of main engine room. Thus, the total damage can be calculated by using the weighting factors ω_1=0.2 and ω_2=0.8 as follows:

$$\begin{aligned} \mathbf{S}_{\mathrm{CODAD}} &= 0.2\mathbf{S}_{\mathrm{CODAD,1}} + 0.8\mathbf{S}_{\mathrm{CODAD,2}} = 0.4158 \\ \mathbf{S}_{\mathrm{CODOG}} &= 0.2\mathbf{S}_{\mathrm{CODOG,1}} + 0.8\mathbf{S}_{\mathrm{CODOG,2}} = 0.3966 \\ \mathbf{S}_{\mathrm{CODAG}} &= 0.2\mathbf{S}_{\mathrm{CODAG,1}} + 0.8\mathbf{S}_{\mathrm{CODAG,2}} = 0.4010 \end{aligned} \tag{54.b}$$

and the global survivability for each architecture is given as

$$\begin{aligned} \mathbf{AM}_{\mathrm{CODAD}} &= 1 - \mathbf{S}_{\mathrm{CODAD}} = 0.5842 \\ \mathbf{AM}_{\mathrm{CODOG}} &= 1 - \mathbf{S}_{\mathrm{CODOG}} = 0.6034 \\ \mathbf{AM}_{\mathrm{CODAG}} &= 1 - \mathbf{S}_{\mathrm{CODAG}} = 0.5989 \end{aligned} \tag{55}$$

5. Conclusions

A range of different potential damage scenarios, including localized structural damage and the failure of critical equipment and systems caused by shock damage, have been considered. After conducting an in-depth damage source analysis, a model combining the fuzzy theory and the analytic hierarchy process (AHP) was selected as the mathematical basis for the proposed method. The analytical model enables the vulnerability of ship propulsion system components, including gas turbines, synchro clutches, and gears, to be determined. The methodology was then applied to evaluate the survivability of a modern naval ship during the initial concept design phase. The main findings of the study are as follows:

(a) The study provides a summary of the damage characteristics and nine types of effects caused by four conventional anti-ship weapons, including missiles, bombs, torpedoes, and mines. The damage process and four damage forms were categorized into fire-induced damage caused by explosion, damage induced by high-speed fragment penetration, high-level shock acceleration damage caused by the underwater explosion shock wave effect, and flooding of power room caused by the naval ship hull off-hull crack.

(b) The five levels of damage (i.e., mean well, minor damage, medium damage, serious damage, and complete loss) can give reasonable descriptions of a propulsion system. In addition, the fifth-order analytic hierarchy process (AHP) structural tree model, which considers both the shock damage and crevasse damage, is a highly efficient method to represent the main damage process in the severe shock environment. Moreover, the fuzzy matrix with a fuzzy membership function using normal distribution types can also separate the fuzzy effects, including the cross points of adjacent damage regions.

(c) The damage evaluation results of the survivability of three propulsion system design types (CODOG, CODAD, and CODAG) for a 3000 T class frigate, as a simplified example of an Oliver Hazard Perry-class frigate, show that this model is intended to be a fast and robust method, which can obtain the damage level of each key part of propulsion system. This enables changes based on the analysis results to be made during the iterative design cycles.

REFERENCES

[1] Makarov, S.O. Discussions of Questions in Naval Tactics. *Annapolis: Naval Institute Press*, 1991, pp 1-65.

[2] Office of the Chief of Naval Operations, *OPNAVINST 9070.1B*. 2017.

[3] Cullis, I. G.; Schofield, J.; Whitby, A. Assessment of blast loading effects - Types of explosions and loading effects. *International Journal of Pressure Vessels and Piping* 2010**,** 87 (9), 493–503. https://doi.org/10.1016/j.ijpvp.2010.07.003

[4] Fujimoto, K.O. 軍艦設計に封する欧洲大戦の教訓. *Journal of Zosen Kiokai* 1921, no. 29, 20–66, (in Japanese)

[5] Cruse, J.H. Conventional Weapons Underwater Explosions. AD-A201814, 1950.

[6] Takashi, Y. 旧海軍艦船の爆弾被害損傷例について--直撃爆弾および至近爆弾による損傷-1. 船の科学 1990, 43 (5), 62–65, 1990 (in Japanese)

[7] Jolliff, J.V. Implementing survivability characteristics into navy ships. *Naval Engineering Journal* 1976, 87 (9), 41–46. https://doi.org/10.1111/j.1559-3584.1976.tb05234.x

[8] Jump, M.E.; Emberson,W.C. Ship Electromagnetic Pulse Survivability Trials. *Naval Engineering Journal* 1991, 103 (3), 136–140. https://doi.org/10.1111/j.1559-3584.1991.tb00944.x

[9] Ball, R.E.; Calvano, C.N. Establishing the Fundamentals of a Surface Ship Survivability Design Discipline. *Naval Engineering Journal* 1994, 106 (1), 71–74. https://doi.org/10.1111/j.1559-3584.1994.tb02798.x

[10] Jim, H.C.; *et al*. Necessity of survivability design technique on Korean naval vessel and its developing guidance. *Journal of Society of Naval Architecture of Korea* 2006, 43 (4), 41–49.

[11] Primorac, B.; Parunov, J. Probabilistic models of reduction in ultimate strength of a damaged ship. *Transactions Of FAMENA* 2015, 39 (2), 55-74.

[12] Nikola, V; Senjanović, I.; Hadžić, N.; Dae, S.C.; Jose L.M.L. Structural integrity of an aged oil tanker converted into the port oil storage. *Transactions Of FAMENA* 2019, 43 (1), 65-77. https://doi.org/10.21278/TOF.43105

[13] Kubit, A..; Jurczak, W..; Trzepiecinski, T.; Faes, K. Experimental and numerical investigation of impact resistance of riveted and RFSSW stringer-Stiffened panels in blunt impact tests. *Transactions Of FAMENA* 2020, 44 (3), 47-58. https://doi.org/10.21278/TOF.44304

[14] Mališ, T.; Šimić Penava, D. The impact of lateral restraint on structural stability of thin-walled C-Cross section column subjected to axial force. *Transactions Of FAMENA* 2017, 41 (3), 13-28. https://doi.org/10.21278/TOF.41302

[15] Vrgoč, A..; Tomičević, Z.; Zaplatić, A.; Hild, F. Damage analysis in glass fibre reinforced epoxy resin via digital image correlation. *Transactions Of FAMENA* 2021, 45 (2), 1-12. https://doi.org/10.21278/TOF.452024020

[16] Said, O.M. Theory and practice of total ship survivability for Ship Design. *Naval Engineering Journal*, 1995, 107 (4), 191–203. https://doi.org/10.1111/j.1559-3584.1995.tb03085.x

[17] Doerry, N. Designing electrical power systems for survivability and quality of service. *Naval Engineering Journal* 2007, 119 (2), 25–34. https://doi.org/10.1111/j.0028-1425.2007.00017.x

[18] Piperakis, A.S. *An integrated approach to naval ship survivability in preliminary ship design*. Ph.D. thesis, University College London, London, 2013.

[19] Kim, K.S.; Hwang, S.Y.; Lee, J.H. Naval ship's susceptibility assessment by the probabilistic density function. *Journal of Computational Design and Engineering* 2014, 1 (4), 266–271. https://doi.org/10.7315/JCDE.2014.026

[20] Liwång, H.; Jonsson, H. Comparison between different survivability measures on a generic frigate. *Transactions of the Royal Institution of Naval Architects Part A: International Journal of Maritime Engineering* 2015, 157 (2): 125–134. https://doi.org/10.3940/rina.ijme.2015.a2.325

[21] Liwång, H. Survivability of an ocean patrol vessel - Analysis approach and uncertainty treatment. *Marine Structures* 2015, 43 (1): 1–21. https://doi.org/10.1016/j.marstruc.2015.04.001

[22] Wright, D. J. The legacy of WWII vulnerability to modern warship design - Lessons learned and forgotten. 2015 Warship - Future Surface Vessels, Bath, UK.

[23] Gualeni, P.; Ruscelli, D.; Bertoldi, G. Application of the Probabilistic Approach to Naval Ships for the Damage Survivability Assessment: An Investigation Case. *Naval Engineering Journal* 2016, 128 (3), 73–86.

[24] Liwång, H. Conditions for a Risk-Based Naval Ship Survivability Approach: A Study on Fire Risk Analysis. *Naval Engineering Journal* 2016, 128 (3), 87–101.

[25] Goodfriend, D.; Brown, A. J. *Exploration of system vulnerability in naval ship concept design*. Journal of Ship Production and Design 2018, 34 (1), 42–58. https://doi.org/10.5957/JSPD.160006

[26] Kovalchuk, S.; Pushnoy, Y.; Shedko, S. Integrated survivability assessment software for ships. *The Transactions of the Krylov State Research Center* 2018, 386 (4), 84–94. https://doi.org/10.24937/2542-2324-2018-4-386-84-94

[27] S. Shedko. Effect of structural protection upon ship survivability. *The Transactions of the Krylov State Research Center* 2020, 391 (1), 128–132. https://doi.org/10.24937/2542-2324-2020-1-391-128-132

[28] Jansen, A.C.; Kana, A. A.; Hopman, J.J. A Markov-based vulnerability assessment for the design of on-board distributed systems in the concept phase. *Ocean Engineering* 2019, 190 (1), 1–11. https://doi.org/10.1016/j.oceaneng.2019.106448

[29] Hoang, N. The application of the AHP method in ship system risk estimation. *Polish Maritime Research* 2009, 16 (1), 78-82. https://doi.org/10.2478/v10012-008-0014-8

[30] Hoang, N. A novel similarity/dissimilarity measure for intuitionistic fuzzy sets and its application in pattern recognition. *Expert Systems with Applications* 2016, 45 (1), 97-107. https://doi.org/10.1016/j.eswa.2015.09.045

[31] Senjanović, I.; Ančić, I.; Magazinović, G.; Alujević, N.; Vladimir, N.; Cho, D.S. Validation of analytical methods for the estimation of the torsional vibrations of ship power transmission systems, *Ocean Engineering*, 2019, 184 (1), 107-120. https://doi.org/10.1016/j.oceaneng.2019.04.016

[32] Senjanović, I.; Hadžić, N.; Murawski, L.; Vladimir, N.; Alujević, N.; Cho,D.S. Analytical procedures for torsional vibration analysis of ship power transmission system, *Engineering Structures*, 2019, 178 (1), 227-244. https://doi.org/10.1016/j.engstruct.2018.10.035

[33] Krstic, I; *et al*. Aircraft performance checking process to achieve an acceptable level of safety through the compliance monitoring function. *Transactions Of FAMENA* 2022, 46 (1), 57-80. https://doi.org/10.21278/TOF.461021620

[34] Ministry of National Defense Republic of Korea. *Joint Investigation Report on the Attack Against the ROK Ship Cheonan*. 2010.

[35] Wang, H.; Zhu, X.; Cheng, Y.S.; Liu, J. Experimental and numerical investigation of ship structure subjected to close-in underwater shock wave and following gas bubble pulse. *Marine Structures* 2014, 39, (1), 90–117. https://doi.org/10.1016/j.marstruc.2014.07.003

[36] Wang, H.; Cheng, Y.S.; Liu, J.; Gan, L. Damage evaluation of a simplified hull girder subjected to underwater explosion load: A semi-analytical model. *Marine Structures* 2016, 45 (1), 43–62. https://doi.org/10.1016/j.marstruc.2015.10.005

[37] Zhang, A.M.; Wei, Z.X.; Wang, S.P.; Feng, L.H. Dynamic response of the non-contact underwater explosions on naval equipment. *Marine Structures* 2011, 24 (4):396–411. https://doi.org/10.1016/j.marstruc.2011.05.005

[38] Bureau of Ships Department. U. S. S. *INDEPENDENCE (CVL22) Torpedo Damage report*. 1945.

[39] Peniston, B. *The Day Frigate Samuel B. Roberts Was Mined Report*. 2015.

[40] Bureau of Ships, Navy Department. *War Damage Report No.* 51*: Destroyer Report - Gunfire, Bomb and Kamikaze Damage*, 1947.

[41] Military Images. *Damage Pictures of HMS Sheffield*. 2007.

[42] Xin, L. *Research on survivability assessment method of shipboard power system*. M.A. thesis, Harbin Engineering University, Harbin, 2011.

[43] Rajendran, R.; Narasimhan, K. Damage prediction of clamped circular plates subjected to contact underwater explosion. *International Journal of Impact Engineering* 2001, 25 (4), 373–386. https://doi.org/10.1016/S0734-743X(00)00051-8

[44] Zhu, X.; Bai, X.; Huang, R.; Liu, R.; Zhao, Y. Crevasse experiment research of plate membrane in vessels subjected to underwater contact explosion. Shipbuilding of China 2003, 44 (1), 46–52.

[45] Yang, C. C.; Peng, X. H. The fuzzy comprehensive assessment of the survivability for warship power. *Journal of Ship Engineering* 1993, 15 (6), 28–34.

[46] Lioness, N. *General Arrangement of Oliver Hazard Perry-class*. 2009.

[47] Huang, K.Z.; Mao, S.P. *Random Method and Application of Fuzzy Mathematics*. Shang Hai, Tongji University Press, 1987.

Submitted: 15.7.2022

Accepted: 20.5.2023

Hao Wang*
China Institute of Marine Technology & Economy, Peking, China
Gan Lin
Wuhan Secondary Ship Design & Research Institute, Wuhan, China
*Corresponding author:
wanghao818489@163.com